Fabrication of porous nickel oxide film with open macropores by electrophoresis and electrodeposition for electrochemical capacitors

Mao-Sung Wu*, Min-Jyle Wang, Jiin-Jiang Jow

Department of Chemical and Materials Engineering, National Kaohsiung University of Applied Sciences, 415, Chien Kung Road, Kaohsiung 807, Taiwan

ARTICLE INFO

ABSTRACT

The electrophoretic deposition of polystyrene sphere monolayer as a template for anodic electrodeposition of interconnected nickel oxide nanoflakes is explored. Result indicates that a nickel oxide film with nanoflakes and open macropores has superior capacitive behavior. A nickel oxide film with interconnected nanoflakes is of great importance for electrochemical capacitors due to the high-specific surface area, fast redox reactions, and shortened diffusion path in solid phase. The open macropores may facilitate the electrolyte penetration and ion migration, therefore increasing the utilization of nickel oxide due to the increased surface area for electrochemical reactions. The specific capacitance of a nickel oxide film with open macropores at a scan rate of $10\,mV\,s^{-1}$ reaches as high as $351\,F\,g^{-1}$, which is 2.5 times higher than that of the bare nickel oxide film ($140\,F\,g^{-1}$).

1. Introduction

The nickel oxide materials have received much research attention due to their potential applications in electrochromic films, optical materials, fuel cell electrodes, photocatalysts, electrochemical capacitors, and batteries, etc. Most of these useful functions depend mainly on their chemical composition, configuration, and structure. The nanostructured nickel oxides have turned out to exhibit better physical and chemical properties than those of their bulk counterparts. There are numerous reports in literature on the synthesis of nanostructured nickel oxides, such as chemical precipitation [1–6], thermal decomposition/oxidation [7–10], hydrothermal process [11–13], surfactant template [14–17], polymer template [18–21], sol–gel method [22–24], and electrodeposition [25–31].

Most of the synthesized nickel oxide materials for electrochemical capacitors are nanopowders. The nickel oxide nanowhiskers or small nanowires fabricated by template are also some of the alternative structures for electrochemical capacitors [30,32]. The nickel oxide nanopowder is often difficult to well disperse in the slurry due to the strong agglomeration of nanopowder. Therefore, it becomes an important challenge for finding innovative ways to fabricate the well-dispersed nickel oxide films at low cost and in a simple manner. To reduce the above-mentioned difficulties, electrochemical deposition, which deposits the active material directly onto the substrate without polymer binder at room temperature,

is used for fabricating the nanostructured nickel oxide films for electrochemical capacitors.

The nanostructured materials are important for electrochemical energy-storage devices because they have high-specific surface area for facilitating the electrochemical redox reactions. Generally, the ion diffusion resistance within the crystal structure of active material dominates the high-rate charging and discharging of an electrode. Diffusion resistance in the solid phase can be mitigated by shortening the diffusion path. Therefore, the nanosized materials can reduce the diffusion resistance effectively. Our previous result has shown that the capacitive behavior of nickel oxide film is considerably affected by the pore size of film [33]. The larger the pore size, the higher the specific capacitance of film. The pore size of nickel oxide film can be increased with decreasing the depositing current density and potential [33]. However, the lower depositing current density (potential) may significantly increase the depositing time, which is unfavorable to the fabrication process. Therefore, in this work, monolayer polystyrene (PS) sphere has been directly fabricated on the stainless steel (SS) substrate by electrophoretic deposition (EPD) as a template for anodic electrodeposition of the nickel oxide film. After removal of the PS template, a nickel oxide film with open macropores can be obtained. The deposited films with and without open macropores have been analyzed in their capacitive behavior.

2. Experimental

The monolayer PS sphere template was assembled by the EPD strategy. The monodispersed PS spheres (with negatively charged surface) of about 200 nm in diameter were suspended in water

* Corresponding author. Tel.: +886 7 3814526; fax: +886 9 45614423.
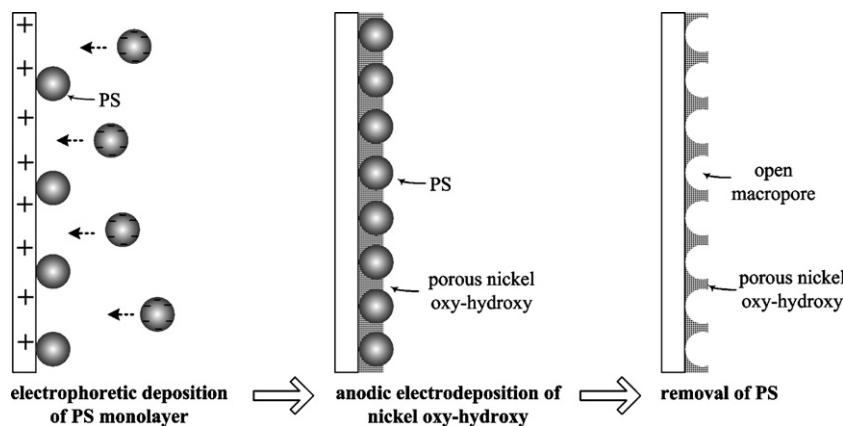*E-mail address:* ms_wu@url.com.tw (M.-S. Wu).

Fig. 1. A schematic of proposed manufacturing process for nickel oxide film with open macropores.

(2.5 wt.%, Alfa Aesar). EPD of the monolayer PS template was carried out by applying a voltage difference of 60 V (Keithley, 2400 source meter) between working (positive electrode, SS, 2 cm × 2 cm) and counter (negative electrode, platinum, 2 cm × 2 cm) electrodes for 30 s. EPD bath was prepared by suspending IPA (50 ml) and PS suspension (16 mg, 2.5 wt.%). Prior to deposition, SS foil was cut into pieces of 2 cm × 2 cm, which were then soaked in acetone and ultrasonically vibrated for 10 min to wash away any contaminants from their surface. De-ionized water was then used to rinse the tailored SS foil in ultrasonic vibration for another 15 min. One side of the SS substrate was exposed opposite a counter electrode, while the other side had been covered with a sheet of polymer insulator (polyethylene terephthalate, Alliance Material S221-H, Taiwan). The distance between working and counter electrodes was kept at 1 cm. After EPD, polymer insulator was removed from the SS substrate, and the PS-coated SS electrode was dried at room temperature for 24 h in air.

The nickel oxide was electrodeposited directly on the PS-coated SS substrate by applying an anodic potential of 1.1 V versus a saturated Ag/AgCl electrode. The plating solution consisted of 0.13 M sodium acetate, 0.13 M nickel sulfate, and 0.1 M sodium sulfate at room temperature [34]. The anodic deposition of nickel oxide was carried out in a three-compartment cell. A saturated Ag/AgCl electrode was used as the reference electrode and a platinum foil with dimension 2 cm × 2 cm was the counter electrode. All chemicals were analytical grade and were used without further purification. The plating solution was stirred by a Teflon stir bar on a magnetic hot plate during the deposition. After deposition, the film was rinsed several times in de-ionized water and then immersed in a toluene solution for 10 min to remove the PS template. The film was annealed at 300 °C for 1 h in air. The amount of deposited films was measured by a microbalance (Mettler, XS105DU) with an accuracy of 0.01 mg and was held almost the same (about 0.5 mg) for each film by adjusting the deposition time.

The capacitive behavior of films was determined by cyclic voltammetry in a three-electrode cell with 1 M KOH electrolyte. The potential was cycled at various scan rates using a potentiostat (CH Instruments, CHI 608) in a range of 0–0.45 V. Galvanostatic charge and discharge were performed by a potentiostat (Princeton Applied Research, EG&G 362) in a range of 0–0.45 V at $10 \, A \, g^{-1}$. All data acquisitions in EG&G 362 were carried out through an interface card (Labjack, U12) with LabVIEW software. AC impedance measurements were performed by means of a potentiostat (CH Instruments, CHI 608) coupled to a frequency response analyzer under the open-circuit condition. An AC perturbation amplitude of 10 mV versus the open-circuit potential was applied in a frequency range from 50 kHz down to 0.1 Hz. The surface morphology

of film was examined with a field-emission electron microscope (FE-SEM, Jeol JEOL-6330) with an accelerating voltage of 3 keV. The zeta potential of PS suspension was measured by a zeta potential analyzer (Brookhaven, 90Plus).

3. Results and discussion

Fig. 1 shows a schematic of the proposed procedure for fabricating a porous nickel oxide film with open macropores. EPD of the PS template is achieved via transport of negatively charged PSs toward a positive electrode (SS substrate) and via deposition of PSs with charge neutralization under an applied electric field. In this work, the formation of PS monolayer on the SS substrate can be achieved by tuning the deposition time. The nickel oxyhydroxy film is deposited anodically on the PS-coated SS substrate in a plating bath of 0.13 M sodium acetate, 0.13 M nickel sulfate, and 0.1 M sodium sulfate. The film formation relies on the oxidation of dissolved Ni^{2+} to Ni^{3+}, which further reacts with the available hydroxide ions from a slightly alkaline electrolyte to form insoluble nickel oxy-hydroxy deposits on the substrate [35]. After deposition, the PS template is dissolved by toluene solution, leading to the formation of open macropores in the nickel oxy-hydroxy film.

Fig. 2 shows the SEM images of deposited nickel oxide film with open macropores after annealing at 300 °C for 1 h. The film is porous and of nanoscaled, the intercrossing network is made up of flaky nickel oxide of thickness ca. 12–16 nm. Interestingly, this film has open macropores about 200 nm in diameter. An average pore size of the flaky film is roughly estimated to be about 40–80 nm observed from SEM image. A porous film with open macropores is believed to be beneficial to the electrolyte penetration, leading to an increase in surface area for electrochemical reactions. The nanoflakes play an important role in enhancing the capacitive behavior of nickel oxide because they have high-specific surface area for redox reactions and shortened diffusion path in solid phase. On the other hand, the pore size of nickel oxide film also plays an important role in electrolyte penetration and migration. A bigger pore is easily accessible by the electrolyte, while a smaller pore is unfavorable to the electrolyte penetration. Therefore, a nickel oxide film with intercrossing nanoflakes and open macropores is in favor of its electrochemical behavior.

The crystal structure of nickel oxide film, which can be determined by a glance angle X-ray diffractometer (XRD), is affect by the annealing temperature and depositing parameter, consequently influences the capacitive behavior of film. Our previous result has shown that a suitable annealing temperature is about 300 °C in terms of the specific capacitance [33]. The annealing temperature is set at 300 °C in this work. The XRD result, which is not shown
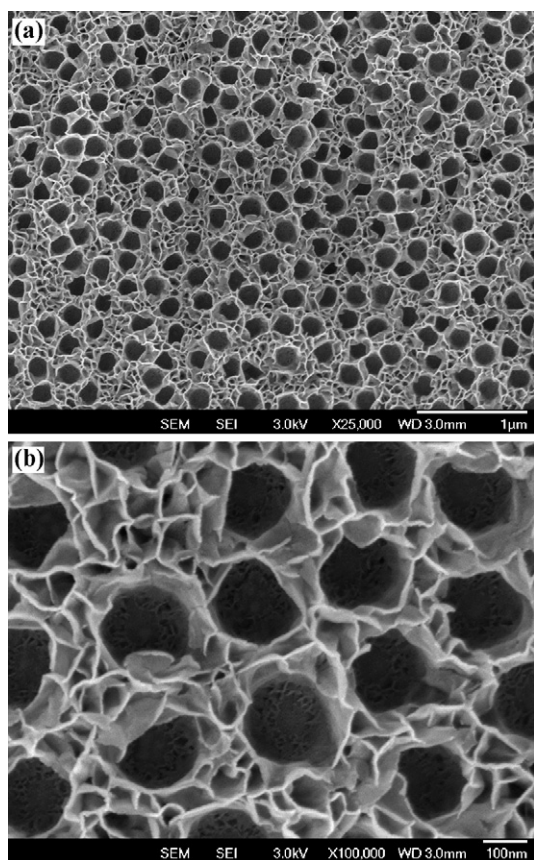
Fig. 2. SEM images of a nickel oxide film with open macropores: (a) low magnification and (b) high magnification.

here, reveals that the diffraction patterns of nickel oxide films with and without open macropores resemble cubic NiO closely.

The electrochemical properties of nickel oxide films are evaluated by means of cyclic voltammogram (CV). Fig. 3 shows the CVs of nickel oxide films with and without open macropores at a scan rate of $25\,mV\,s^{-1}$. If the upper limit potential is lower than 0.3 V, the CVs show a roughly rectangular mirror image with respect to the zero-current line, which represents an electrical double-layer capacitive behavior of films. If the upper limit potential is higher than 0.3 V, the CVs correspond to a redox capacitor. Through redox
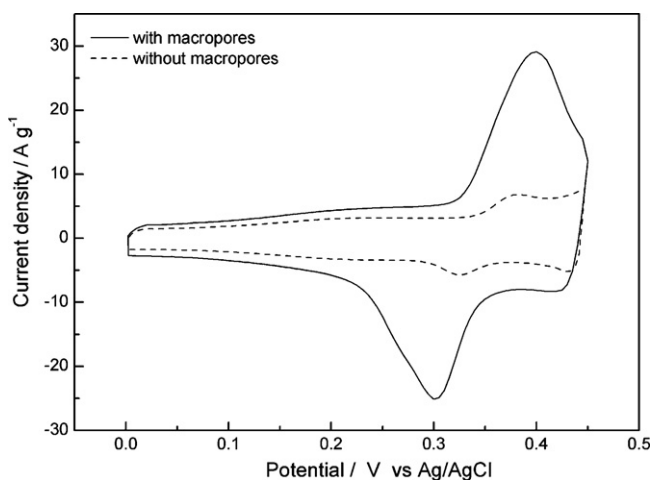

Fig. 3. Cyclic voltammograms of the nickel oxide films with and without open macropores at a scan rate of $25\,mV\,s^{-1}$.
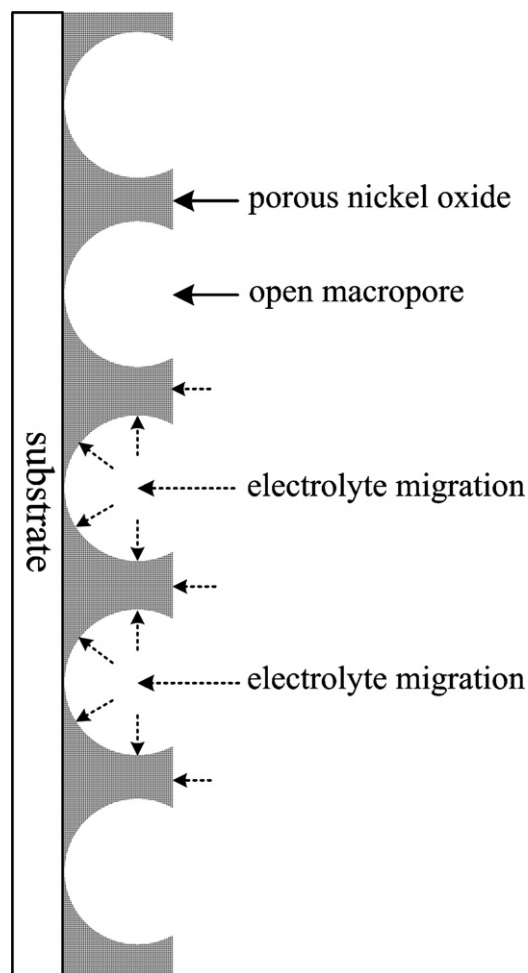

Fig. 4. A schematic of proposed strategy for enhancing the capacitive behavior of a nickel oxide film.

reactions, much more capacitance can be stored in the bulk of nickel oxide than in the electrical double layer. Clearly, the oxidation and reduction peaks are observed at 0.37 V (oxidation) and 0.3 V (reduction), respectively. The redox couple of nickel oxide films in alkaline solution can be expressed as follows [36–38]

$$NiO + OH^- \leftrightarrow NiOOH + e^- \qquad (1)$$

Obviously, the peak current of a nickel oxide film with open macropores is much higher than that of film without macropores. The higher the response current density, the larger the specific capacitance of film. This reflects that a porous film with bigger pores (macropores) may facilitate the electrolyte penetration, leading to a decrease in the electrolyte diffusion (migration) resistance. Fig. 4 shows a schematic of the proposed strategy for enhancing the capacitive behavior of a nickel oxide film. A nickel oxide film having open macropores can shorten the ion migration and diffusion paths, leading to an increase in the effective surface area for electrochemical reaction. While a nickel oxide film without open macropores, the migration and diffusion resistances of ions are pronounced, especially in the region near the SS substrate.

The capacitance response of an electrode during high-rate charging and discharging (or high-rate CV scan) is an important factor for achieving practical application in the electrochemical capacitor because of the high power demand from portable electronic power tools and electric vehicles. An electrode, due to the Faradaic reaction and diffusion resistances, has a lower capacitance when the scan rate is high. Fig. 5 shows the measured specific capac-
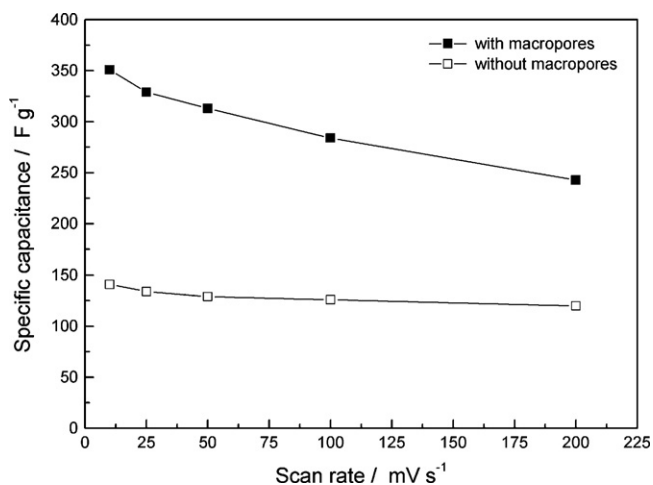
Fig. 5. Specific capacitance variations of the nickel oxide films with and without open macropores associated with the CV scan rate.

Fig. 6. Nyquist plots of the nickel oxide films with and without open macropores.

itances of the nickel oxide films with and without open macropores at various scan rates. The specific capacitance (C) of films is calculated by dividing half the integrated area of the CV curve by the scan rate to obtain the charge (Q) and by subsequently dividing Q by the width of the potential window (ΔV) [39]

$$C = \frac{Q}{\Delta V} = \frac{1}{v\,\Delta V} \int_0^{0.45} i\,dV \tag{2}$$

where i is the current density ($A\,g^{-1}$), ΔV is the potential window (V), V is the applied potential (V), and v is the scan rate ($V\,s^{-1}$).

As can be seen from Fig. 5, both films have higher specific capacitance at low scan rate than those at high scan rate. A nickel oxide film with open macropores has a specific capacitance of $351\,F\,g^{-1}$ at a low scan rate of $10\,mV\,s^{-1}$, and the value reduces to $243\,F\,g^{-1}$ (70% capacitance of $10\,mV\,s^{-1}$) at a high scan rate of $200\,mV\,s^{-1}$. On the other hand, a nickel oxide film with open macropores exhibits higher capacitance compared with a film without macropores even at higher scan rates, possibly because this film has a large electroactive area on the surface layer of the nickel oxide nanoflakes for high-rate charging and discharging. A small decrease in specific capacitance with increasing scan rate also indicates the high power characteristics of a nickel oxide film with open macropores. The calculated specific capacitance of a nickel oxide film with open macropores at a scan rate of $10\,mV\,s^{-1}$ reaches $351\,F\,g^{-1}$, which is 2.5 times higher than that of film without macropores ($140\,F\,g^{-1}$).

High capacity retention at high scan rate also reflects that the Faradaic reaction occurring on the active sites of nickel oxide surface is fast enough to maintain the current response during high-rate scanning. Possibly, the configuration of interconnected nanoflakes provides much more paths for electron conduction, and the flake-like structure shortens the ion diffusion paths within the bulk of solid nickel oxide. In addition, the macroporous structure benefits electrolyte penetration and provides larger surface area for charge-transfer reactions. Therefore, the capacitive behavior of a nickel oxide film with open macropores is significantly improved.

The capacitive behavior of a porous electrode is affected not only by the specific surface area for electrolyte accessibility but also by the electrical conductivity for electron transfer. Usually, the specific surface area of the electrode materials is measured by means of BET technique using nitrogen gas to relate the capacitance of the materials. However, it is difficult to deposit the requisite quantity of material needed for BET analysis in this work. Instead,
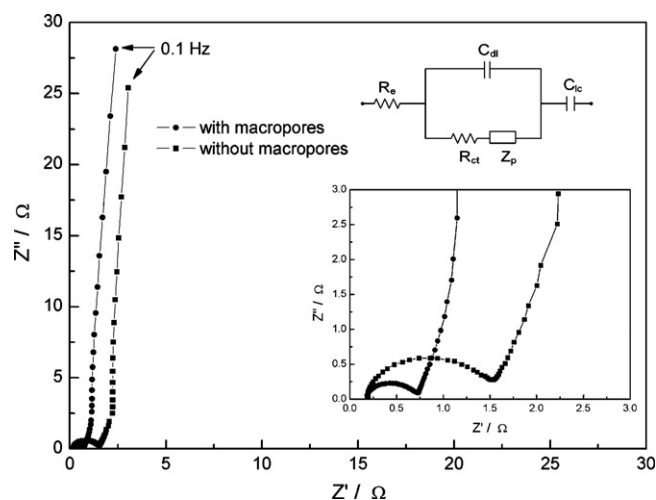
we use AC impedance technique to investigate the effect of open macropores on the capacitive behavior of nickel oxide film. The AC impedance is a well-developed technique generally used to predict the behavior of electrochemical capacitor, and to determine the parameters affecting the performance of an electrode, including its conductivity, charge-transfer properties, diffusion properties, etc. Fig. 6 shows the Nyquist plots of nickel oxide films with and without open macropores. The corresponding equivalent circuit for impedance analysis is shown in the inset of Fig. 6. At very high frequencies, the intercept at real part (Z') is a combinational resistance of electrolyte resistance, intrinsic resistance of substrate, and contact resistance at the active material/current collector interface (R_e) [40]. This value is almost the same for both films (deduced from the enlarged figure shown in the inset of Fig. 6). A major difference is the semicircle in the high-frequency range, which corresponds to the charge-transfer resistance (R_{ct}) caused by the Faradaic reaction and the double-layer capacitance (C_{dl}) on the nickel oxide surface. Charge separation at micropores is represented by the transmission line Z_p which relates to the distributed electronic and ionic conductivity and double-layer capacitance inside the micropores; C_{lc} is the limit capacitance [41]. The calculated charge-transfer resistances for the films with and without open macropores are about 0.5 and $1.2\,\Omega$, respectively. The charge-transfer resistance of nickel oxide film having open macropores is much lower than that of the bare film. The charge-transfer resistance is related to the electroactive surface area of film materials for the Faradaic reaction to occur. The larger the electroactive surface area, the lower the charge-transfer resistance of film. Accordingly, a nickel oxide film having open macropores exhibits a larger electroactive surface area possibly due to an increase in the electrolyte accessible area. A nickel oxide film without open macropores shows a high charge-transfer resistance, reflecting that the specific capacitance mainly comes from the EDL capacitance rather than the Faradaic capacitance. This explains that the CV current response of nickel oxide film without macropores shows a roughly rectangular mirror image with respect to the zero-current line as shown in Fig. 3.

Fig. 7 shows the galvanostatic charge/discharge curves of nickel oxide films with and without open macropores at a current density of $10\,A\,g^{-1}$: limit potentials 0 and 0.45 V versus Ag/AgCl. The charging time (from 0 to 0.45 V) and discharging time (from 0.45 to 0 V) are almost the same, implying a high reversibility of the Faradaic reaction taking place on the nickel oxide surface. The charging time and discharging time of a film with open macropores in each cycle are much higher than those of a film without open macropores, reflecting that the open macropores can facilitate the capacitive
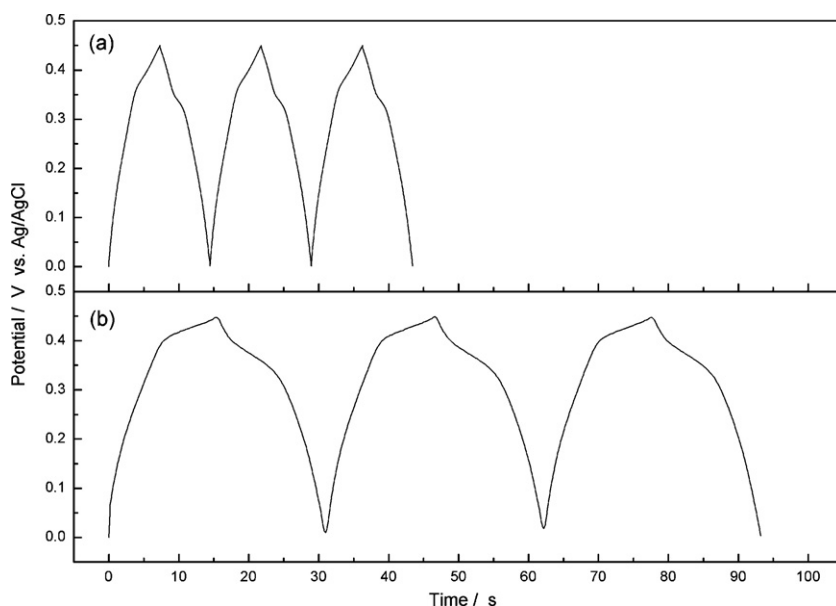
Fig. 7. Galvanostatic charge/discharge curves of the nickel oxide films at a current density of 10 A g^{-1}: (a) a film without open macropores and (b) a film with open macropores.

behavior of a nickel oxide film. The specific capacity (Q) of nickel oxide films during galvanostatic test is calculated according to the equation

$$Q = \frac{i\Delta t}{w} \tag{3}$$

where w is the mass of active material and i is the galvanostatic current applied for time Δt.

The cycle-life stability of nickel oxide films is carried out by galvanostatic charging/discharging at 10 A g^{-1}. Fig. 8 shows the relationship between capacitance retention and cycle number of both deposited films. Two curves are almost the same, meaning that the effect of open macropores on the cycle-life stability of a nickel oxide film is very small. The capacitance retention of both films increases at the beginning of the 750 charging/discharging cycles, and then stabilizes for ongoing cycles. The capacitance retentions of both films after 3000 cycles remain almost unchanged, reflecting a high durability of nickel oxide films for electrochemical capacitor application in alkaline solution.
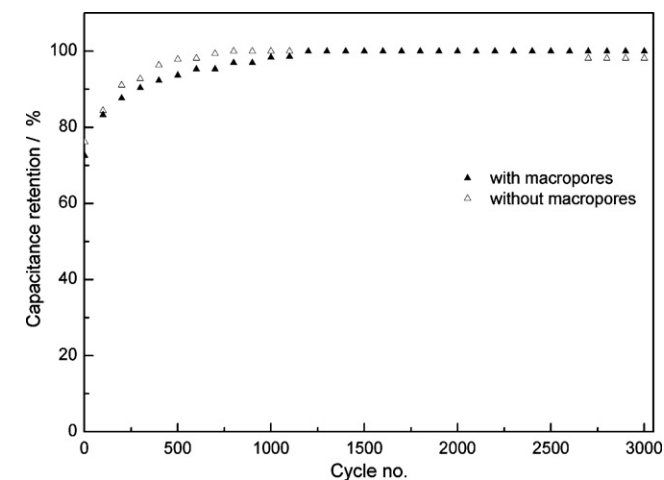
4. Conclusion

The porous nickel oxide film with interconnected nanoflakes and open macropores has been successfully prepared by anodic electrodeposition of oxy-hydroxide onto PS template adsorbed on a SS substrate by electrophoresis. The formation of PS sphere monolayer can be achieved via transport of negatively charged PSs toward SS substrate and via deposition of PSs with charge neutralization under an applied electric field. The electrochemical performance of the nickel oxide film turns out to be significantly affected by the open macropores. The specific capacitance of nickel oxide film with open macropores is much higher than that of film without open macropores in all scan rates. Possibly, a highly porous film with bigger open pores offers large surface area for fast charge storage and redox reactions and is capable of delivering high power, so it can be discharged/recharged at high rates. A nickel oxide film with open macropores exhibits high capacity and stable capacity retention during cycling, and therefore is suitable for long-time applications in KOH solution.

Fig. 8. Capacitance retention of the nickel oxide films with and without open macropores during galvanostatic charge/discharge cycling.

References

[1] J.W. Lang, L.B. Kong, W.J. Wu, M. Liu, Y.C. Luo, L. Kang, J. Solid State Electrochem. 13 (2009) 333.
[2] L. Wu, Y. Wu, H. Wei, Y. Shi, C. Hu, Mater. Lett. 58 (2004) 2700.
[3] X. Wang, H. Luo, H. Yang, P.J. Sebastian, S.A. Gamboa, Int. J. Hydrogen Energy 29 (2004) 967.
[4] L. Xiang, X.Y. Deng, Y. Jin, Scripta Mater. 47 (2002) 219.
[5] Y.L. Zhao, J.M. Wang, H. Chen, T. Pan, J.Q. Zhang, C.N. Cao, Int. J. Hydrogen Energy 29 (2004) 889.
[6] M.S. Wu, H.H. Hsieh, Electrochim. Acta 53 (2008) 3427.
[7] T. Nathan, A. Aziz, A.F. Noor, S.R.S. Prabaharan, J. Solid State Electrochem. 12 (2008) 1003.
[8] X. Li, X. Zhang, Z. Li, Y. Qian, Solid State Commun. 137 (2006) 581.
[9] Y. Wang, J. Zhu, X. Yang, L. Lu, X. Wang, Thermochim. Acta 437 (2005) 106.
[10] T. Ohmori, K. Tachikawa, K. Tsuji, K. Anzai, Int. J. Hydrogen Energy 32 (2007) 5094.
[11] X.M. Liu, X.G. Zhang, S.Y. Fu, Mater. Res. Bull. 41 (2006) 620.
[12] Z.H. Liang, Y.J. Zhu, X.L. Hu, J. Phys. Chem. B 108 (2004) 3488.

[13] Y.Y. Xi, D. Li, A.B. Djurisic, M.H. Xie, K.Y.K. Man, W.K. Chan, Electrochem. Solid-State Lett. 11 (2008) D56.
[14] H.J. Liu, T.Y. Peng, D. Zhao, K. Dai, Z.H. Peng, Mater. Chem. Phys. 87 (2004) 81.
[15] X.Y. Guan, J.C. Deng, Mater. Lett. 61 (2007) 621.
[16] T. Ahmad, K.V. Ramanujachary, S.E. Lofland, A.K. Ganguli, Solid State Sci. 8 (2006) 425.
[17] W. Xing, F. Li, Z.F. Yan, H.M. Cheng, G.Q. Lu, Int. J. Nanosci. 3 (2004) 321.
[18] D. Wang, C. Song, Z. Hu, X. Fu, J. Phys. Chem. B 109 (2005) 1125.
[19] D. Tao, F. Wei, Mater. Lett. 58 (2004) 3226.
[20] D.W. Wang, F. Li, H.M. Cheng, J. Power Sources 185 (2008) 1563.
[21] M.W. Xu, S.J. Bao, H.L. Li, J. Solid State Electrochem. 11 (2007) 372.
[22] Y. Wu, Y. He, T. Wu, T. Chen, W. Weng, H. Wan, Mater. Lett. 61 (2007) 3174.
[23] Q. Li, L.S. Wang, B.Y. Hu, C. Yang, L. Zhou, L. Zhang, Mater. Lett. 61 (2007) 1615.
[24] T. Sreethawong, S. Chavadej, S. Ngamsinlapasathian, S. Yoshikawa, Colloid Surf. A-Physicochem. Eng. Aspects 296 (2007) 222.
[25] V. Srinivasan, J.W. Weidner, J. Electrochem. Soc. 144 (1997) L210.
[26] E.E. Kalu, T.T. Nwoga, V. Srinivasan, J.W. Weidner, J. Power Sources 92 (2001) 163.
[27] K.W. Nam, E.S. Lee, J.H. Kim, Y.H. Lee, K.B. Kim, J. Electrochem. Soc. 152 (2005) A2123.
[28] E.B. Castro, S.G. Real, L.F. PinheiroDick, Int. J. Hydrogen Energy 29 (2004) 255.
[29] M.S. Wu, Y.A. Huang, C.H. Yang, J.J. Jow, Int. J. Hydrogen Energy 32 (2007) 4153.
[30] K.R. Prasad, N. Miura, Appl. Phys. Lett. 85 (2004) 4199.
[31] M.S. Wu, C.H. Yang, Appl. Phys. Lett. 91 (2007) 033109.
[32] Y.G. Wang, Y.Y. Xia, Electrochim. Acta 51 (2006) 3223.
[33] M.S. Wu, Y.A. Huang, C.H. Yang, J. Electrochem. Soc. 155 (2008) A798.
[34] D. Tench, L.F. Warren, J. Electrochem. Soc. 130 (1983) 869.
[35] M.S. Wu, C.H. Yang, M.J. Wang, Electrochim. Acta 54 (2008) 155.
[36] K.C. Liu, M.A. Anderson, J. Electrochem. Soc. 143 (1996) 124.
[37] C. Natarajan, H. Matsumoto, G. Nogami, J. Electrochem. Soc. 144 (1997) 121.
[38] P. Delichere, S. Joiret, A. Hugot-Le Goff, K. Bange, B. Hetz, J. Electrochem. Soc. 135 (1988) 1856.
[39] N. Nagarajan, H. Humadi, I. Zhitomirsky, Electrochim. Acta 51 (2006) 3039.
[40] J. Gamby, P.L. Taberna, P. Simon, J.F. Fauvarque, M. Chesneau, J. Power Sources 101 (2001) 109.
[41] A.D. Fabio, A. Giorgi, M. Mastragostino, F. Soavi, J. Electrochem. Soc. 148 (2001) A845.